Available online at www.sciencedirect.com
SCIENCE DIRECT®
International Journal of Heat and Mass Transfer 49 (2006) 4124–4131
International Journal of HEAT and MASS TRANSFER
www.elsevier.com/locate/ijhmt

Analytical solution for a transient, three-dimensional temperature distribution due to a moving laser beam

Guillermo Araya [a,*], Gustavo Gutierrez [b]

[a] Department of Mechanical, Aeronautical and Nuclear Engineering, Rensselaer Polytechnic Institute, Troy, NY 12180-3590, United States
[b] Department of Mechanical Engineering, University of Puerto Rico-Mayagüez, PR 00681-9045, United States

Received 11 August 2005; received in revised form 23 March 2006
Available online 5 June 2006

Abstract

This paper presents an analytical solution of the transient temperature distribution in a finite solid when heated by a moving heat source. The analytical solution is obtained by solving the transient three-dimensional heat conduction equation in a finite domain by the method of separation of variables (SOV). Meanwhile previous studies focus on analytical solutions for semi-infinite domains, here an analytical solution is provided for a finite domain. The non-homogeneous equation is solved by using the Laplace transform for a unit impulse and then convoluted with the actual heat source. Two different distributions are used: a Gaussian distribution and a spatially uniform plane heat source.

Keywords: Temperature distribution; LAM; Analytical solution; Moving heat source

1. Introduction

Lasers are being increasingly employed in material processing due to their ability to generate a highly concentrated thermal energy. One important application is in Laser Assisted Machining (LAM), a relatively recent technique for machining brittle ceramic materials by, first, heating and softening the material with a laser beam, without reaching its melting point and; finally, cutting the workpiece by means of a tool as in the traditional process. In this way, the damage of the workpiece and tool is minimized.

Jaeger [1] and Carslaw and Jaeger [2] presented solutions for solving a broad range of moving heat source cases (band, square or rectangular) in some manufacturing and tribological applications using the heat source method. According to Hou and Komanduri [3], this technique would be more appropriately termed *the method of superposition of temperature field of individual heat sources*. Rosenthal [4] pioneered the application of the theory of moving point and moving line heat sources for welding.

Woo and Cho [5] found an analytical solution of the temperature distribution in surface hardening processes using a moving laser beam as a heat source, for a three-dimensional domain of finite thickness, but infinite along the laser path and transversal directions. The heat source was assumed to take the form of a rectangular constant energy density, obtaining fairly good agreements with the performed experiments.

Modest and Abakians [6] solved the heat conduction problem due to a moving heat source with a Gaussian distribution in an infinite domain of semi-infinite thickness at quasi-steady state. They considered CW and pulsed laser irradiation, obtaining an exact solution for the latter case. It was concluded that a simple integral method with one-dimensional conduction (normal to the surface) could be applied instead of the exact solutions as long as the non-dimensional laser speed (the laser speed multiplied by laser radius and divided by the thermal diffusivity of material) be higher than 10. Additionally, for the pulsed laser irradiation, the non-dimensional period (the laser speed multiplied

* Corresponding author.
E-mail address: arayaj@rpi.edu (G. Araya).

0017-9310/$ - see front matter © 2006 Elsevier Ltd. All rights reserved.
doi:10.1016/j.ijheatmasstransfer.2006.03.026

Nomenclature

C_P	specific heat	t	time
CW	continuous wave	T	temperature
L_x	domain dimension in the x-direction	TEM	transverse electromagnetic mode
L_y	domain dimension in the y-direction	T_0	ambient temperature
L_z	domain dimension in the z-direction	U	velocity of the laser beam
k_T	workpiece thermal conductivity	x, y, z	Cartesian coordinates
h	convection coefficient		
q_0	heat flow absorbed by the workpiece	*Greek symbols*	
q''	heat flux	α_T	thermal diffusivity
q'''	heat generation	ρ	density

by the pulse laser period and divided by the laser radius) must be much lower than the non-dimensional velocity in order to neglect lateral conduction.

Komanduri and Hou [7] obtained a general solution for the laser surface hardening process using a disk heat source with a pseudo-Gaussian heat intensity distribution in a semi-infinite steel workpiece of finite width. They inferred that this exact analytical solution provided a better insight into the physical process of laser transformation hardening of steels than the semi-empirical equations developed by Steen and Courtney [8] based on the regression analysis of the experimental data.

Stephenson et al. [9] developed a transient, three-dimensional analytical model for predicting cutting tool temperature through the separation of variable method, considering a fixed heat source on the surface of the insert. Comparison with measured temperatures showed good agreement.

Experimental data and numerical modeling regarding temperature distribution in a sample of silicon nitride are encountered [10–13] at different laser powers and cutting speeds in a LAM process. According to these investigations, the temperature near the cutting tool location must be in excess of approximately 1000 °C to successfully machine silicon nitride material.

Most of the analytical solutions encountered in the literature are based on semi-infinite domains and quasi-steady states for a constant source speed. To the best of our knowledge, there is not in the literature a transient, three-dimensional analytical solution for a complete finite domain describing the temperature evolution due to a space-dependent moving heat source. For this reason, the present paper attempts to fill the gap above-mentioned in order to validate a previous numerical model, analyze the boundary effects, investigate start-up effects and evaluate the influence of parameters involved in the LAM process, mainly power and speed of the heat source.

2. Mathematical modeling

Consider a laser beam source used to pre-heat a parallelepiped workpiece of finite dimension L_x, L_y and L_z (see Fig. 1). As the laser progresses with a velocity U, the heat from the source penetrates further into the workpiece.

The following assumptions are considered:

- Heat losses by radiation are negligible as compared to the intensity of the incident laser beam (Gutierrez and Araya [14], Modest and Abakians [15]).
- Thermal properties are considered constant and evaluated at an average temperature.

With the above assumptions, the governing equation is the transient heat conduction equation, that written in terms of $\theta = T - T_0$, yields:

$$\frac{1}{\alpha_T}\frac{\partial\theta}{\partial t} = \frac{\partial^2\theta}{\partial x^2} + \frac{\partial^2\theta}{\partial y^2} + \frac{\partial^2\theta}{\partial z^2} + \frac{q'''(x,y,z,t)}{k_T} \tag{1}$$

where k_T and α_T are the thermal conductivity and thermal diffusivity of the workpiece, respectively, and $q'''(x,y,z,t)$ is the heat generation source term.

2.1. Heat source modeling

The heat source term $q'''(x,y,z,t)$ is considered as a laser beam of temporal *continuous wave* (CW) and spatially modeled by assuming two different distributions: a spatially uniform plane heat source and a Gaussian distribution (corresponding to the theoretical TEM_{00} mode of the laser). TEM comes from the acronym transverse elec-

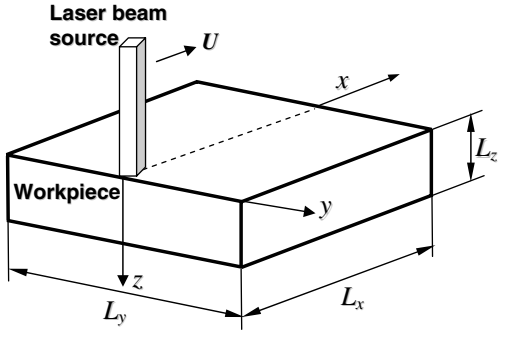

Fig. 1. Schematic of the laser beam and the finite workpiece.

tromagnetic mode, specifying the number of nodes generated by a slight misalignment of the mirrors located in the laser cavity. Fig. 2 shows some transverse modes and the simplest mode, TEM_{00}, is considered in this paper.

The purpose is to compare the temperature profiles calculated by employing both heat source models with the same net power and the same heating area, since a constant heat flux model would diminish enormously the calculation effort.

The spatially uniform distribution takes the form of a rectangular constant energy density:

$$q'' = \begin{cases} \frac{q_0}{4RS} & @\ z = 0, \quad Ut < x < Ut + 2R, \text{ and } -S < y < +S \\ 0 & \text{otherwise} \end{cases} \tag{2}$$

Here, q_0 is the heat flow absorbed by the workpiece, R and S are the half-size of the laser beam along x and y, respectively. Finally, U is the laser beam velocity.

The irradiance distribution of the Gaussian TEM_{00} beam can be described as follows:

$$I(r) = I_0 e^{-kr^2/r_0^2} \tag{3}$$

where I_0 is the intensity at the center of the spot [W/m^2], k is the constant (in general, a value of 2 is used for a Gaussian model).

The radial coordinate r is related to the Cartesian coordinates x and y, through:

$$r = \sqrt{x^2 + y^2}$$

$$r_0 = \sqrt{\frac{4}{\pi}(RS)} : \text{beam waist radius(m)}$$

In this way, the circular area for the Gaussian distribution is the same as the rectangular area for the uniform heat flux distribution.

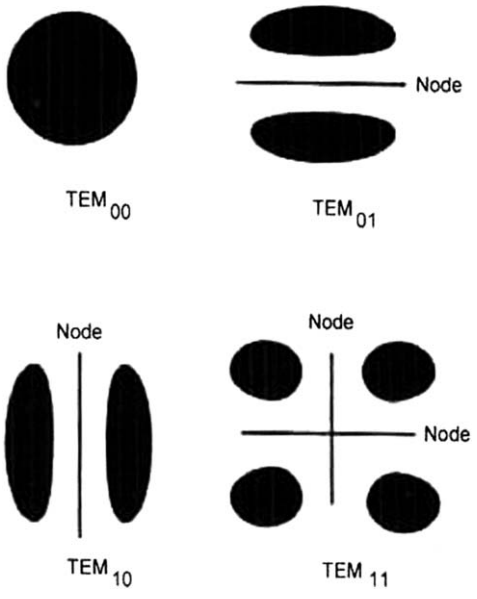

Fig. 2. Different transversal modes in a laser spot.

The Gaussian heat flux distribution is imposed as:

$$q'' = \begin{cases} I_0 e^{-k(x^2+y^2)/r_0^2} & @\ z = 0, \quad Ut - r_0 < x < Ut + r_0, \text{ and} \\ \quad -\sqrt{r_0^2 - x^2} < y < +\sqrt{r_0^2 - x^2} \\ 0 \quad \text{otherwise} \end{cases} \tag{4}$$

In both cases, the volumetric heat generation is defined as $q''' = q''\delta(z)$, being $\delta(z)$ the Dirac delta function.

2.2. Initial and boundary conditions

Boundary conditions at the six faces of the parallelepiped domain and an initial condition have to be provided (@ $t = 0$, $\theta = 0$).

Insulated conditions were imposed at $x = 0$ and $y = 0$ (condition of symmetry), meanwhile constant surface conditions were considered at $x = L_x$, $y = L_y/2$ and $z = L_z$. The main reason of selecting Dirichlet conditions at faces $x = L_x$, $y = L_y/2$ and $z = L_z$ can be summarized as follows: the numerical results obtained in a previous investigation [14] showed that the above mentioned workpiece faces always reached ambient temperature no matter which boundary condition was established, due to the extremely concentrated heating effect of the laser source and dimensions of the workpiece. Two different boundary conditions are analyzed at the top surface: Case 1 considers an insulated condition except on the heating zone powered by the laser, and Case 2 regards a convection boundary condition, instead.

The non-homogeneous boundary value problem of Eq. (1) can be solved by assuming that $\theta(x, y, z, t)$ is expressed as a series expansion of the eigenfunctions:

$$\theta(x, y, z, t) = \sum_i \sum_j \sum_k \Theta_{ijk}(t) X_i(x) Y_j(y) Z_k(z) \tag{5}$$

The eigenvalues and eigenfunctions have the form:

$$X_i(x) = \cos(\alpha_i x), \quad \alpha_i = \frac{2i+1}{2L_x}\pi, \quad i = 0, 1 \ldots n \tag{6}$$

$$Y_j(y) = \cos(\beta_j y), \quad \beta_j = \frac{2j+1}{L_y}\pi, \quad j = 0, 1 \ldots n \tag{7}$$

Case 1 $$Z_k(z) = \cos(\gamma_k z), \quad \gamma_k = \frac{2k+1}{2L_z}\pi, \quad k = 0, 1 \ldots n \tag{8}$$

Case 2 $$Z_k(z) = \cos(\gamma_k z) + \frac{h}{k_T \gamma_k}\sin(\gamma_k z) \tag{9}$$

where $\tan(\gamma_k L_z) = \frac{-k_T \gamma_k}{h}$ is the eigencondition. Here, α^2, β^2, γ^2 are the separation constants.

It is possible to express the non-homogeneous term q''' as a linear combination of the eigenfunctions:

$$q''' = \sum_i \sum_j \sum_k \phi_{ijk}(t) X_i(x) Y_j(y) Z_k(z) \tag{10}$$

Multiplying Eq. (10) side-by-side by the eigenfunctions, integrating over the whole domain and making use of the orthogonality property of the eigenfunctions:

$$\int_0^{L_x}\int_{-L_y/2}^{L_y/2}\int_0^{L_z} q'''X_i(x)Y_j(y)Z_k(z)\mathrm{d}x\,\mathrm{d}y\,\mathrm{d}z = \phi_{ijk}(t)\int_0^{L_x}X_i^2(x)\mathrm{d}x\int_{-L_y/2}^{L_y/2}Y_j^2(y)\mathrm{d}y\int_0^{L_z}Z_k^2(z)\mathrm{d}z = \phi_{ijk}(t)\frac{L_xL_y}{4}\int_0^{L_z}Z_k^2(z)\mathrm{d}z \quad (11)$$

Since q''' is known, the function $\phi_{ijk}(t)$ is also known. The triple integral on the left hand of Eq. (11) is solved differently according to the two heat source distributions considered. Also, integration of the eigenfunctions $Z_k(z)$ depends on the case analyzed: insulated or convective conditions at the top surface.

2.3. Spatially uniform plane heat source and insulated top surface

In this case, integration of Eq. (11) is straightforward and an analytical expression for $\phi_{ijk}(t)$ can be obtained:

$$\phi_{ijk}(t)=\frac{q_0}{4RS}\frac{8}{L_xL_yL_z}\int_0^{L_x}X_i(x)\mathrm{d}x\int_{-L_y/2}^{L_y/2}Y_j(y)\mathrm{d}y\int_0^{L_z}\delta(z)Z_k(0)\mathrm{d}z \quad (12)$$

Integrating the eigenfunctions;

$$\int_0^{L_x}X_i(x)\mathrm{d}x=\int_{X_s}^{X_s+2R}\cos(\alpha_i x)\mathrm{d}x=\left.\frac{\sin(\alpha_i x)}{\alpha_i}\right|_{X_s}^{X_s+2R} \quad (13)$$

where X_s is the source position each instant of time, i.e., the product of the source velocity, U, by time, t.

$$\int_{-L_y/2}^{L_y/2}Y_j(y)\mathrm{d}y=\int_{-S}^{S}\cos(\beta_j y)\mathrm{d}y=\frac{2}{\beta_j}\sin(\beta_j S) \quad (14)$$

$$\int_0^{L_z}\delta(z)Z_k(0)\mathrm{d}z=\int_0^{L_z}\delta(z)\left[\cos(0)+\frac{h}{k_T\gamma_k}\sin(0)\right]\mathrm{d}z=\int_0^{L_z}\delta(z)\mathrm{d}z=1 \quad (15)$$

In expression (15), the same result is obtained for Cases 1 and 2 because the sinusoidal function is null at the surface, i.e., at $z=0$.

Finally, $\phi_{ijk}(t)$ is determined by substituting Eqs. (13) and (14) into Eq. (12):

$$\phi_{ijk}(t)=\frac{4q_0}{RSL_xL_yL_z\beta_j\alpha_i}\sin(\beta_j S)[\sin(\alpha_i(X_s+2R))-\sin(\alpha_i(X_s))] \quad (16)$$

Substituting Eq. (16) into Eq. (10) and inserting it into Eq. (1) together with Eq. (5), an ordinary differential equation for $\Theta_{ijk}(t)$ is obtained:

$$\frac{1}{\alpha_T}\frac{\mathrm{d}\Theta_{ijk}}{\mathrm{d}t}=-(\alpha_i^2+\beta_j^2+\gamma_k^2)\Theta_{ijk}+\frac{\phi_{ijk}}{k_T} \quad (17)$$

Defining $\omega_{ijk}=(\alpha_i^2+\beta_j^2+\gamma_k^2)\alpha_T$ and $\Omega_{ijk}(t)=\frac{\alpha_T}{k_T}\phi_{ijk}(t)$, Eq. (17) results;

$$\frac{\mathrm{d}\Theta_{ijk}}{\mathrm{d}t}+\omega_{ijk}\Theta_{ijk}=\Omega_{ijk}(t) \quad (18)$$

With the following initial condition:

$$\theta(x,y,z,0)=\sum_i\sum_j\sum_k\Theta_{ijk}(0)X_iY_jZ_k=0 \quad (19)$$

Since $X_i(x), Y_j(y)$ and $Z_k(z)$ are not zero for arbitrary values of x, y and z, it follows that $\Theta_{ijk}(0)=0$. For solving Eq. (18), we consider first an impulse applied at $t=0$;

$$\frac{\mathrm{d}\Theta_{ijk}}{\mathrm{d}t}+\omega_{ijk}\Theta_{ijk}=\delta(t) \quad (20)$$

Taking the Laplace transform to Eq. (20):

$$sH(s)+\omega_{ijk}H(s)=1\Rightarrow H(s)=\frac{1}{s+\omega_{ijk}} \quad (21)$$

where $H(s)$ is the transfer function. Performing the corresponding inverse Laplace transform of (23), $h(t)=\ell^{-1}[H(s)]=\mathrm{e}^{-\omega_{ijk}t}$. Now, superimposing the function $\Omega_{ijk}(t)$, the response is the convolution of $h(t)$ with $\Omega_{ijk}(t)$:

$$\Theta_{ijk}(t)=h(t)*\Omega_{ijk}(t)=\int_0^t h(t-\tau)\cdot\Omega_{ijk}(\tau)\mathrm{d}\tau \quad (22)$$

For the uniform heat flux distribution, the integral (22) results:

$$\Theta_{ijk}(t)=-2\alpha_T q_0\frac{(\omega_{ijk}A+\mathrm{e}^{-\omega_{ijk}t}B+\alpha_i UC)}{D} \quad (23)$$

where

$$A=\cos(\beta_jS+\alpha_iUt+2\alpha_iR)-\cos(\beta_jS-\alpha_iUt-2\alpha_iR)+\cos(\beta_jS-\alpha_iUt)+\cos(\beta_jS+\alpha_iUt)$$

$$B=\omega_{ijk}[\cos(\beta_jS-2\alpha_iR)-\cos(\beta_jS+2\alpha_iR)]-2\alpha_iU\sin(\beta_jS)[\cos(2\alpha_iR)-1]$$

$$C=\sin(\beta_jS+\alpha_iUt+2\alpha_iR)+\sin(\beta_jS-\alpha_iUt-2\alpha_iR)-\sin(\beta_jS-\alpha_iUt)-\sin(\beta_jS+\alpha_iUt)$$

$$D=\beta_j\alpha_iL_xL_yL_zSRk_T\left(\alpha_T^2\alpha_i^4+2\alpha_T^2\alpha_i^2\beta_j^2+2\alpha_T^2\alpha_i^2\gamma_k^2+\alpha_T^2\beta_j^4+2\alpha_T^2\beta_j^2\gamma_k^2+\alpha_T^2\gamma_k^4+\alpha_i^2U^2\right)$$

The temporal function (23) together with the eigenfunctions (6)–(9) constitutes the temperature distribution due to a moving constant heat flux dictated by Eq. (5).

2.4. Gaussian distribution and insulated top surface

A similar procedure is followed; nevertheless, the heat power now depends on the x and y coordinates, and cannot be removed out of the integral (11). For the insulated top surface case, Eq. (11) can be written as follows;

$$\int_{x_c-r_0}^{x_c+r_0}\int_{-\sqrt{r_0^2-(x-x_c)^2}}^{\sqrt{r_0^2-(x-x_c)^2}} I_o\mathrm{e}^{-k\frac{[(x-x_c)^2+y^2]}{r_o^2}}\cos(\alpha_i x)\cos(\beta_j y)\mathrm{d}x\mathrm{d}y=\phi_{ijk}(t)\frac{L_xL_yL_z}{8} \quad (24)$$

where x_c represents the x-coordinate of the heating circle center on the surface and is given by the product Ut. Since the laser is moving, the limits of integration in the x-direction are changing. To obtain an expression for $\phi_{ijk}(t)$, the surface integral is computed numerically for each mode i, j at each time instant.

2.5. Convective top surface

For accounting the heat loss due to convection in the top surface, the eigenvalues must now be calculated from the tangential function, and the computation of the integral (11) by means of the eigenfunction (9).

3. Results and discussion

The analytical solution is tested for pre-heating a workpiece of silicon nitride, whose thermophysical properties are summarized in Table 1 (Incropera and DeWitt [16], Touloukian et al. [17]). Dimensions of the workpiece are $0.04\ \text{m} \times 0.02\ \text{m} \times 0.00625\ \text{m}$ along x, y and z-directions, respectively.

3.1. Spatially uniform plane heat source and insulated top surface

In this case, the dimensions of the square heat source are $1\ \text{mm} \times 1\ \text{mm}$, a net power of 50 W and a laser speed of 0.1 m/s. Since the temperature gradients are very steep near the heat source, many eigenvalues have to be used and the Fourier series becomes expensive computationally. After conducting a convergence test, it was determined that a number of 800 eigenvalues in each direction was enough to obtain an accurate solution.

Fig. 3 shows a typical two-dimensional temperature profile in the workpiece surface. As can be seen, the affected zone by the laser source is extremely concentrated.

Comparison of the analytical solution with a previous numerical model developed by Gutierrez and Araya [14] is depicted in Figs. 4–6 along x, y and z-directions, respectively. The laser beam is at 0.75 L_x and in all temperature profiles a good agreement can be appreciated. Regarding start-up effects, it is established that a distance of approximately three source lengths is necessary to reach the quasi-steady state condition.

Influence of lateral boundaries ($y = \pm L_y/2$) can be neglected if they are located farther than, at least, one source length from the laser beam path; this means that

Table 1
Thermophysical properties silicon nitride (Si_3N_4)

Melting point (°C)	1900
Density (kg/m^3)	2400
Specific heat C_p (J/kg °C) @ 1000 °C	1278.96
Thermal conductivity (W/m°C) @ 1000 °C	5.91
Thermal diffusivity (m^2/s) @ 1000 °C	1.9×10^{-6}

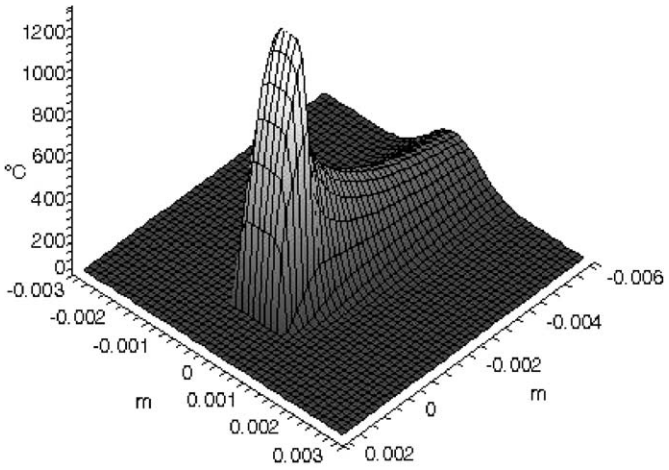

Fig. 3. Two-dimensional temperature profile on the workpiece surface.

the solid may be considered as a semi-infinite domain. Thus; if the domain of interest is large enough in the x and y-directions, in such a way that the influence of lateral boundaries can be neglected; the present analytical solution for a finite region approaches the solution for an infinite domain (in x and y) of finite thickness introduced by Woo and Cho [5], according to Fig. 7. The latter solution is much simpler and cheaper to compute than the present one; however, for small domains or heating points next to the boundaries, the influence of lateral faces may posses an important impact on maximum temperatures. Also, the effect of the workpiece thickness on the peak temperature is observed in Fig. 7, as comparison of the present solution with a solution obtained by Carslaw and Jaeger [2] for an infinite domain (in x and y) of semi-infinite thickness

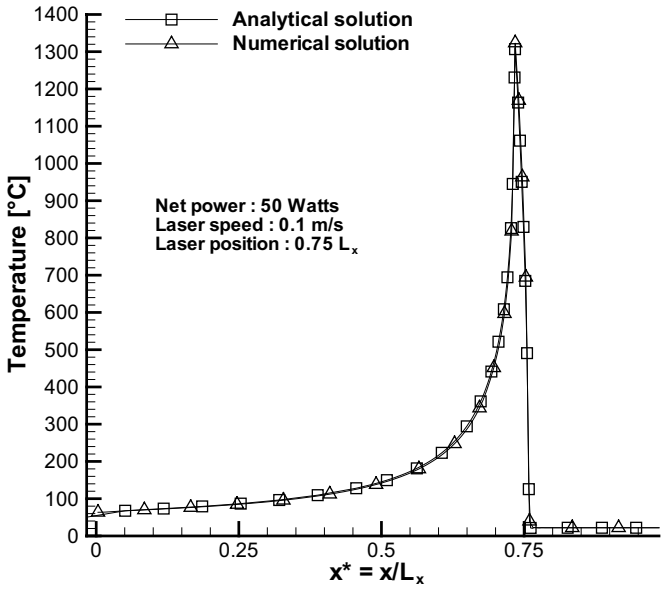

Fig. 4. Comparison of the analytical solution with numerical predictions [14] along the x-direction over the surface ($z = 0$) and at the plane of symmetry ($y = 0$).

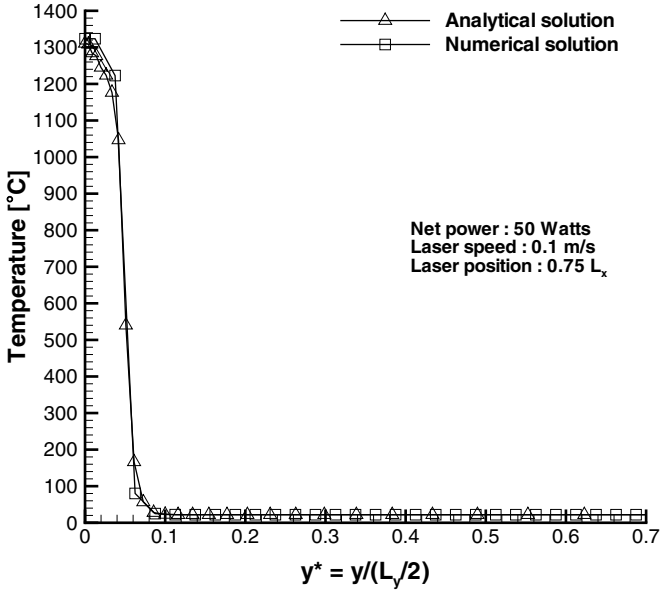

Fig. 5. Comparison of the analytical solution with numerical predictions [14] in the y-direction over the surface ($z = 0$).

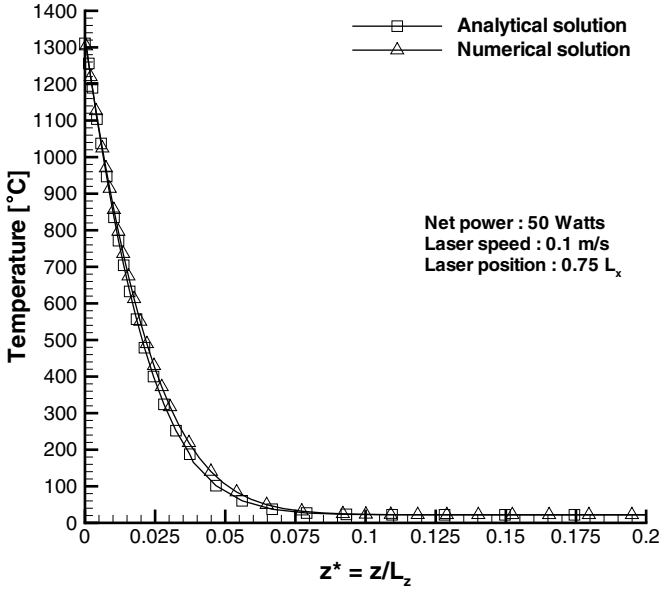

Fig. 6. Comparison of the analytical solution with numerical predictions [14] in the z-direction at the plane of symmetry ($y = 0$) just under the laser spot.

(in z). It was necessary to increase twelve times the original workpiece thickness to obtain a top surface temperature similar to that of a semi-infinite solid by the Carslaw and Jaeger [2] solution.

Figs. 8 and 9 show the trend of temperature profiles behind the laser position along the y and z-directions. It is appreciated a rapid decrease of temperatures together with a 'smoothing' process of peak values. For instance, the peak temperature diminished more than three times

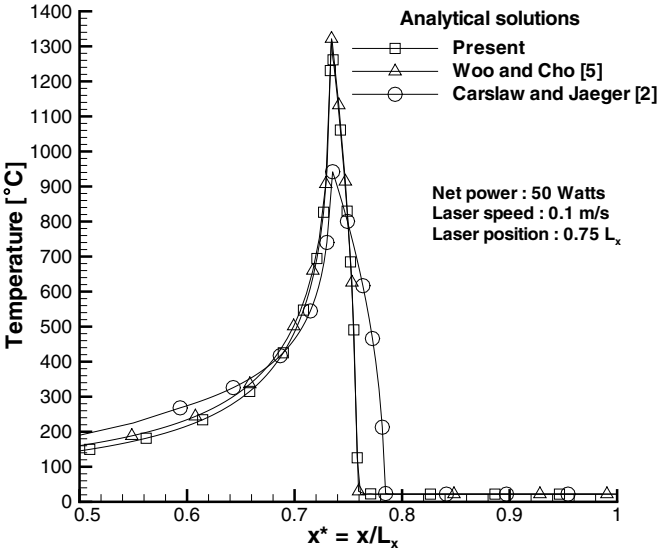

Fig. 7. Comparison of the different analytical solutions for a moving square heat source according to the assumed domain.

at only 2 mm (0.7 L_x) behind the laser spot position (0.75 L_x).

3.2. Gaussian distribution and insulated top surface

For comparison, temperature profiles for Gaussian and constant heat flux distributions of the laser beam are calculated by using a net power of 50 W and a laser speed of 0.1 m/s. The integral in the left-hand side of Eq. (24) is solved numerically for each mode i, j at each time instant to obtain an expression for $\phi_{ijk}(t)$. In this case, it is established that 150 eigenvalues are good enough for reaching convergence.

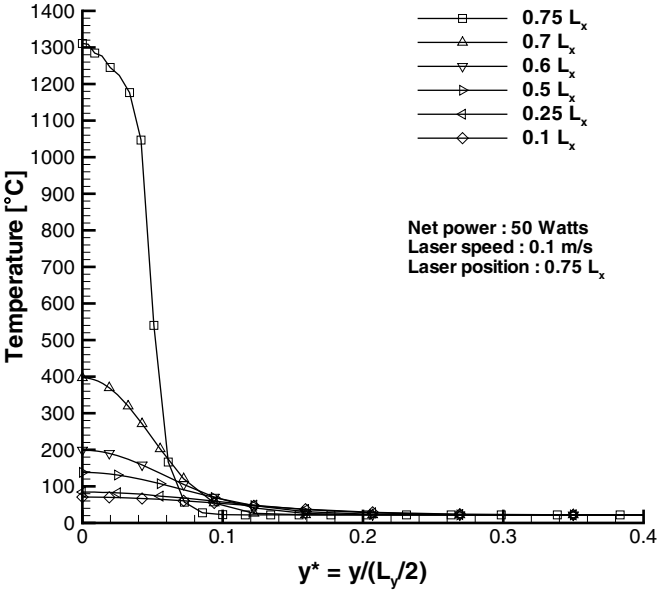

Fig. 8. Temperatures profiles along the y-direction, over and behind the laser spot position.

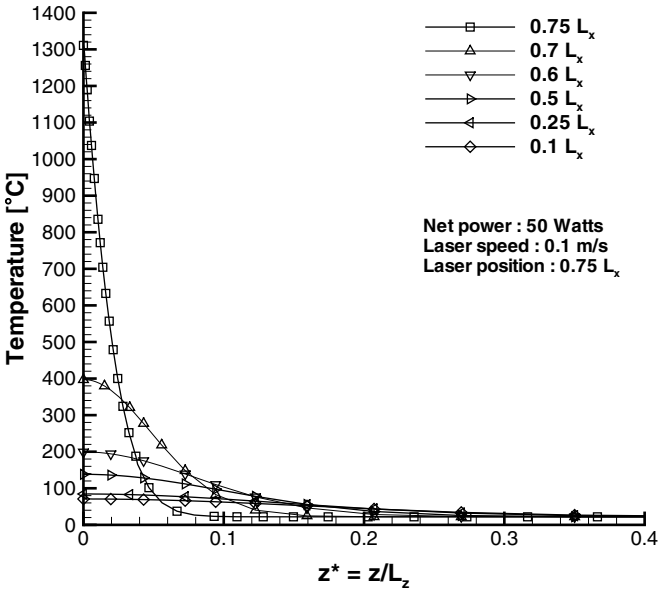

Fig. 9. Temperatures profiles along the z-direction, over and behind the laser spot position.

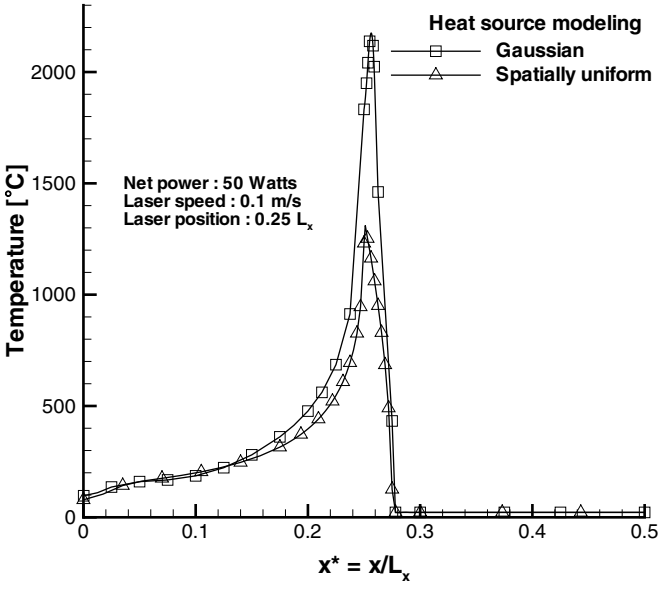

Fig. 10. Gaussian vs. spatially uniform heat source modeling.

For the above conditions, the maximum surface temperature obtained by using a constant heat flux model was 1311 °C, meanwhile the Gaussian distribution generated a peak of 2175 °C. Therefore considering the last value as the more realistic one, the difference in peak temperatures is around 40%. In Fig. 10, it is observed both temperature profiles when the laser source is at 0.25 L_x and remarkable discrepancies exist near the location of the concentrated heat source; however, both temperature profiles present similar trends far from the source. In summary, it is not appropriate to consider a laser beam as a constant heat flux, even at similar heating surfaces and input powers, due to the considerable disparities obtained in peak temperatures.

Table 2
Necessary parameters for reaching the softening temperature in silicon nitride

Net heat power (W)	50	100	200	300
Required speed (m/s)	0.28	0.72	2.15	3.8

A specific application of the solution encountered in a LAM process is showed in Table 2, which exhibits the required laser speed and absorbed heat power to reach a surface temperature of approximately 1000 °C, considering a Gaussian distribution for the laser beam. This temperature (1000 °C) allows silicon nitride to become softer; improving the production time, minimizing the damage of the workpiece and resulting in a higher tool life [10–13].

All cases were run in a processor Apple X server with 2 GB of memory. Comparison of CPU times required by the present analytical solution and a previous numerical simulation [14] indicated the supremacy, as expected, of the latter one. CPU time of the analytical solution with Gaussian model is approximately ninety times longer than the CPU time of a spatially uniform heat source model. On the other hand, the ratios between CPU times of the analytical (spatially uniform and Gaussian distributions) to numerical solutions are, respectively, 7×10^4 and 6.5×10^6.

3.3. Convective top surface

The majority of laser assisted machining processes utilizes a gas assist jet to protect the laser focusing optic from machining debris; therefore, considering a forced convective top surface (Case 2) is more realistic. Since there was no previous research on the forced convection coefficients in LAM processes, the coefficient selected is that used in laser hardening processes [5], which are similar thermal processes: 184 W/m^2 K.

Differences in the surface temperatures for the forced convection case were roughly 2.5% when compared with the insulated case, utilizing one of the required power-speed combinations to reach the softening temperature (1000 °C), i.e., 50 W and 0.28 m/s.

Convection condition requires finding the eigenvalues from a transcendental equation that introduces additional numerical efforts without gaining much accuracy.

4. Conclusions

In this study; an analytical solution, for describing the transient temperature distribution induced by a moving heat source in a finite domain, is determined.

Two models for the laser source are analyzed: spatially uniform plane and Gaussian distributions, obtaining remarkable discrepancies in peak temperatures.

Boundary effects were estimated, having the workpiece thickness the most significant influence on surface temper-

atures. On the other hand, surface temperature reached its maximum value (quasi-steady state) in a very short distance, around three source lengths.

Finally, forced convection effects are practically negligible and can be ignored for the sake of simplicity without impact in the accuracy of the solution.

Acknowledgements

Dr. Gustavo Gutierrez and Mr. Guillermo Araya would like to thank the University of Puerto Rico-Mayagüez for the support to this work.

References

[1] J.C. Jaeger, Moving source of heat and the temperature at sliding contacts, Proc. Roy. Soc. NSW 76 (1942) 203–224.
[2] H.S. Carslaw, J.C. Jaeger, Conduction of Heat in Solid, Oxford University Press, 1959.
[3] Z.B. Hou, R. Komanduri, General solutions for stationary/moving plane heat source problems in manufacturing and tribology, Int. J. Heat Mass Transfer 43 (2000) 1679–1698.
[4] D. Rosenthal, The theory of moving sources of heat and its application to metal treatments, Trans. ASME 80 (1946) 849–866.
[5] H.G. Woo, H.S. Cho, Three-dimensional temperature distribution in laser surface hardening processes, Proc. Instn. Mech. Engrs. 213 (Part B) (1999) 695–712.
[6] M.F. Modest, H. Abakians, Heat-conduction in a moving semi-infinite solid subjected to pulsed laser irradiation, J. Heat Transfer Trans. ASME 108 (3) (1986) 597–601.
[7] R. Komanduri, Z. B Hou, Thermal analysis of the laser surface transformation hardening process, Int. J. Heat Mass Transfer 44 (2001) 2845–2862.
[8] W.M. Seen, C.H.G. Courtney, Surface heat treatment of EN 8 steel using a 2 kW continuous wave CO_2 laser, Met. Technol. (1979) 456–462.
[9] D.A. Stephenson, T.C. Jen, A.S. Lavine, Cutting tool temperatures in contour turning: transient analysis and experimental verification, J. Manuf. Sci. Eng. ASME Trans. 119 (1997) 494–501.
[10] S. Lei, Y.C. Shin, Experimental investigation of thermo-mechanical characteristics in laser-assisted machining of silicon nitride ceramics, J. Manuf. Sci. Eng. 123 (2001) 639–646.
[11] J.C. Rozzi, Experimental and theoretical evaluation of the laser assisted machining of silicon nitride. Ph.D. Thesis. Purdue University, West Lafayette, IN, 1997.
[12] J.C. Rozzi, F.E. Pfefferkorn, F.P. Incropera, Y.C. Shin, Experimental evaluation of the laser-assisted machining of silicon nitride ceramics, ASME J. Manuf. Sci. Eng. 122 (2000) 666–670.
[13] J.C. Rozzi, F.E. Pfefferkorn, F.P. Incropera, Y.C. Shin, Transient, three-dimensional heat transfer model for the laser assisted machining of a silicon nitride ceramic: Part I- comparison with measured surface temperature histories, Int. J. Heat Mass Transfer 43 (2000) 1409–1424.
[14] G. Gutierrez, G. Araya, Temperature distribution in a finite solid due to a moving laser beam, Proceedings of IMECE, ASME Congress at Washington, D.C., IMECE2003-42545, 2003.
[15] M.F. Modest, H. Abakians, Evaporative cutting of a semi-infinite body with a moving CW laser, J. Heat Transfer 108 (1986) 602–607.
[16] F.P. Incropera, D.P. DeWitt, Fundamentals of Heat and Mass Transfer, fourth ed., Wiley, 1996.
[17] Y.S. Touloukian, R.W. Powell, C.Y. Ho, P.G. Klemens, Thermophysical properties of matter, TPRL Inc., West Lafayette, Report No. TPRL 2128, 1970.